Weekly Report

SCSB/CISESS
Cooperative Research Program Division (CoRP)
STAR/NESDIS
National Oceanic and Atmospheric Administration (NOAA)

Submitted by: Hugo Berbery
Prepared by: Debra Baker
Date of Submission: 9/4/2020

Products and Applications

MiRS Precipitation Rate Product for Hurricane Laura: Hurricane Laura struck the southwest Louisiana coast in the early morning hours of August 27th with peak winds likely in excess of 150 mph. It caused extensive damage, due to both winds and a storm surge which likely exceeded 9 feet. Thanks to NOAA's dual ATMS-bearing satellites, Suomi-NPP and NOAA-20, and NOAA's Microwave Integrated Retrieval System (MiRS), the storm's devastating potential was well-monitored as soon as it passed by the island of Hispanola.

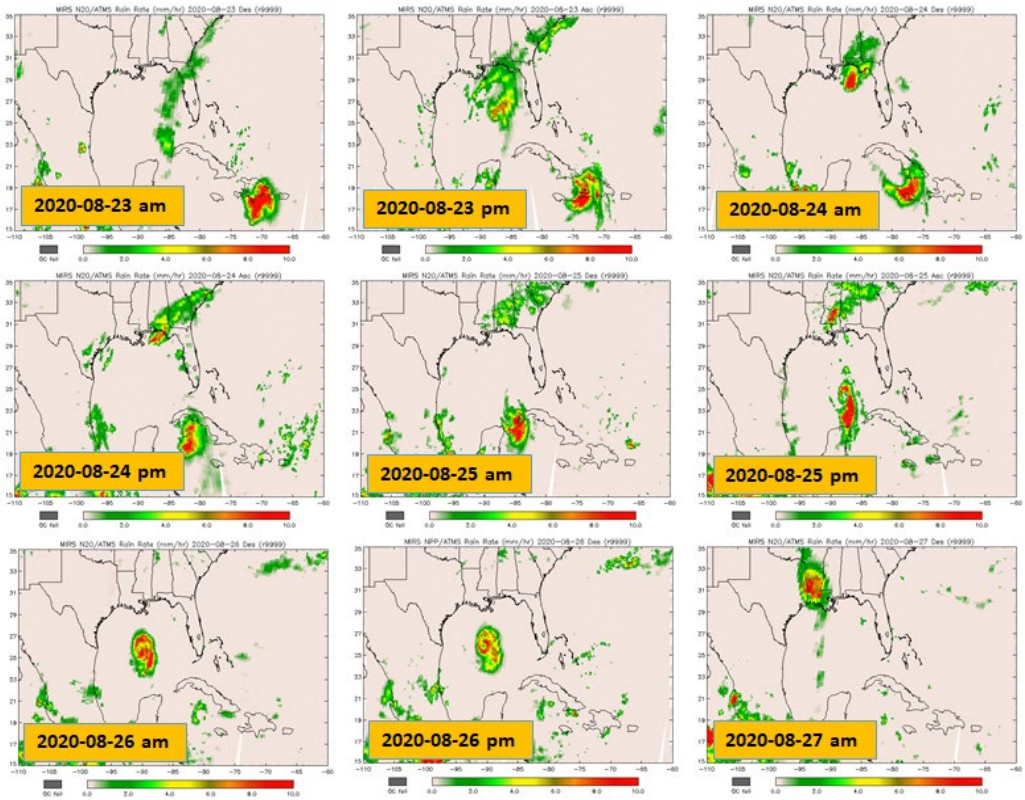

***Figure**: Sequence of MiRS retrieved rain rates from NOAA-20/ATMS from 23-27 August, 2020. Both Hurricane Laura and Tropical Storm Marco are depicted with microwave precipitation rates exceeding 10-15 mm/hour.*

Among the many retrieval products generated by MiRS is the precipitation rate. The sequence shown above contains the NOAA-20/ATMS rain rates retrieved every 12 hours as the satellite made another pass over the storm from August 23rd to the morning of the 27th, when landfall occurred. The rain rates vary in intensity but increase as the storm approaches the coast, consistent with its intensification to a Category 4 hurricane. At some points the distinct hurricane eye is depicted. Also noteworthy on August 23-24, the remnants of Tropical Storm Marco can be seen passing over the Mississippi and Alabama coasts.

(*POC: Christopher Grassotti, christopher.grassotti@noaa.gov, Funding: JSTAR)*

Publications

Cloud Particles over the Desert: CISESS-MD and SCSB scientists Yalei You, Ralph Ferraro, Scott Rudlosky, Heshun Wang, and collaborators from NASA, Sorbonne Université (France), New York City College of Technology, and Indian Institute of Science have a new article just published in the August 28th issue of *Geophysical Research Letters*. This study for the first time showed that raindrop emission is the primary cloud particle signature over desert terrain by analyzing observations from two spaceborne radars and two spaceborne radiometers. Low surface emissivity supports the use of liquid raindrop emission as the primary signature over desert surfaces. In these regions, the surface rain rate better correlates with the liquid raindrop emission signal than with the scattering induced by ice further aloft, suggesting a new potential for improving rainfall estimation over deserts by exploiting the liquid raindrop emission signature.

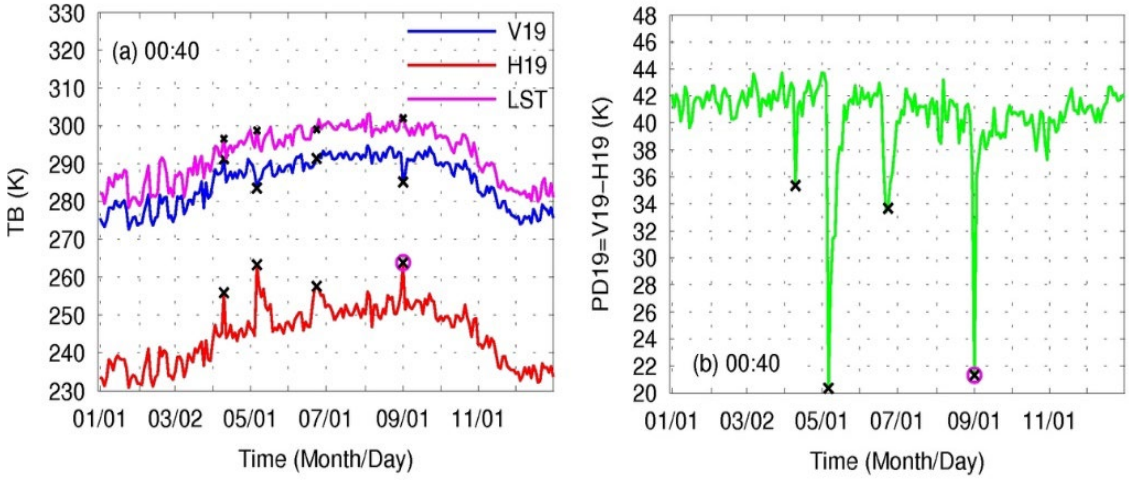

Figure: *(a) Time series at the location of (21.5–21.75°N,14.5–14.75°E) in the Sahara desert around midnight (00:40) for V19, H19, and Land Surface Temperature (LST). (b) Same as (a) except for PD19 (V19-H19). The black crosses indicate the four occasions on 10 April 2009, 7 May 2009, 24 June 2009, and 1 September 2009. The purple circle on panels (a) and (b) indicates that CloudSat CPR observed surface rainfall with radar reflectivity of −4.1 dBZ on 1 September 2009.*

You, Yalei, S. Joseph Munchak, **Ralph Ferraro,** Karen Moh, Christa Peters-Lidard, Catherine Prigent, Sarah Ringerud, **Scott Rudlosky, Heshun Wang,** Hamidreza Norouzi, and Satya Prakash (2020). Raindrop signature from microwave radiometer over deserts. *Geophysical Research Letters*, 47,e2020GL088656. https://doi.org/10.1029/2020GL088656.

(*POC: Yalei You, yyou@umd.edu, Funding: JPSS PGRR)*

Celebrating 40 Years of AVHRR: T. Smith is a co-author on a new paper accepted for publication in *Bulletin of the American Meteorology Society*. The paper is led by S. Kalluri and includes several other members of STAR, including ASPB's A. Heidinger and J. Key. The paper gives an overview of the Advanced Very High Resolution Radiometer (AVHRR) and how it has contributed to satellite remote sensing over the past 40 years. This includes changes and improvements in instruments over time and a summary of some important products developed using AVHRR data. Products include a vegetation index, measures of global cloudiness, atmospheric aerosol estimates, and surface temperature estimates. For example, the figure shows AVHRR-derived aerosol optical thickness before and after the Mt. Pinatubo eruption in 1991.

The two figures below from the article show monthly mean aerosol optical thickness in AVHRR Band 1 over the oceans during May (top) and July (bottom) 1991. Mt. Pinatubo erupted on June 15, 1991 and the volcanic ash circled the globe in 21 days (Stowe et al. 1992). Data from National Center for Environmental Information (Zhao 2017).

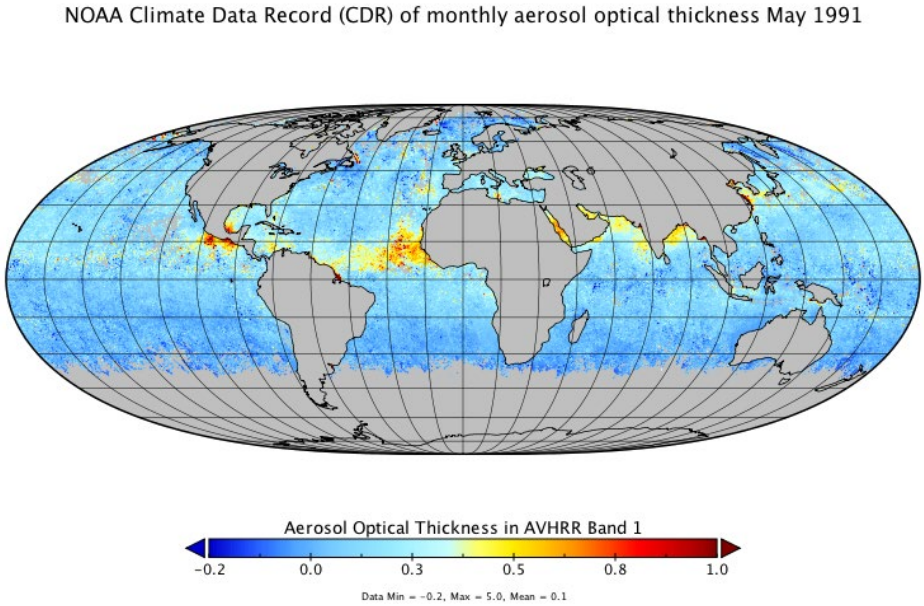

NOAA Climate Data Record (CDR) of monthly aerosol optical thickness July 1991

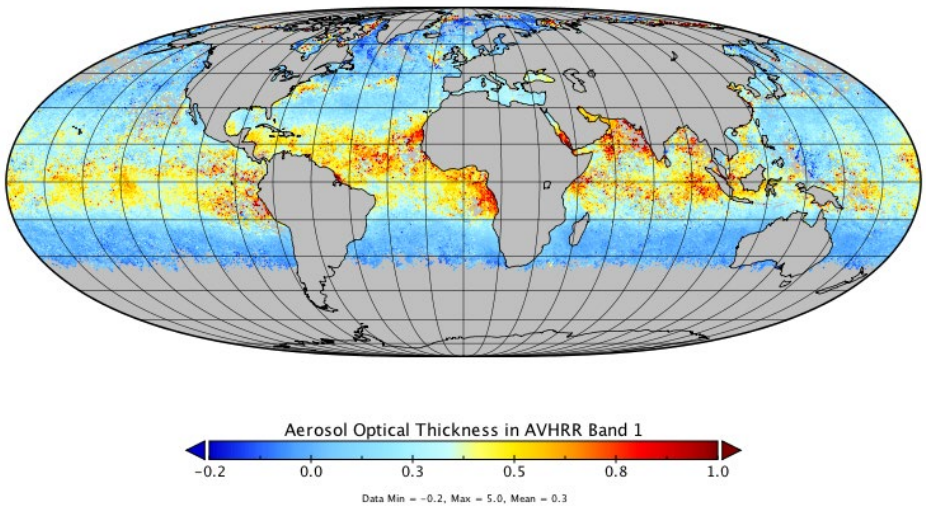

Kalluri, Satya, Changyong Cao, Andy Heidinger, Alexander Ignatov, Jeff Key, and **Thomas Smith**: The advanced very high resolution radiometer: contributing to Earth observations for over forty years. (Accepted for publication in *Bull. Amer. Met. Soc.*)

(*POC: T. Smith, tom.smith@noaa.gov, Funding: PDRA)*

Training and Education

Summer Intern Applies Machine Learning to Snowfall Prediction: Alan Goldfarb from the University of Southern California was one of the three CISESS Summer Interns. He worked with CISESS Scientist Cezar Kongoli on a project to apply machine learning to algorithms for predicting snowfall. He started with satellite measurements of naturally emitted radiation at 13 different combinations of frequency and polarization. Observed snowfall was represented by a categorical variable, snowcode, where a value of 1 represented snowfall and a value of 0 represented no snowfall. To come up with a predictive model, he compared four different modeling methods: logistic regression, discriminant analysis, neural networks, and decision trees. He used the classification rate as the criteria to evaluate the performance of each model. His analysis found that some advanced decision trees produced the most accurate models, with classification rates above 85%. Most models indicate that combining low and high frequencies offers the best predictive ability and vertically polarized radiation is a better predictor than horizontally polarized radiation. Specifically, TB176V, TB183V, TB23V, and TB19V were the best predictors when used together. He provided us with a full written report of his work, which is available on request from CISESS (please email drb@umd.edu for a copy).

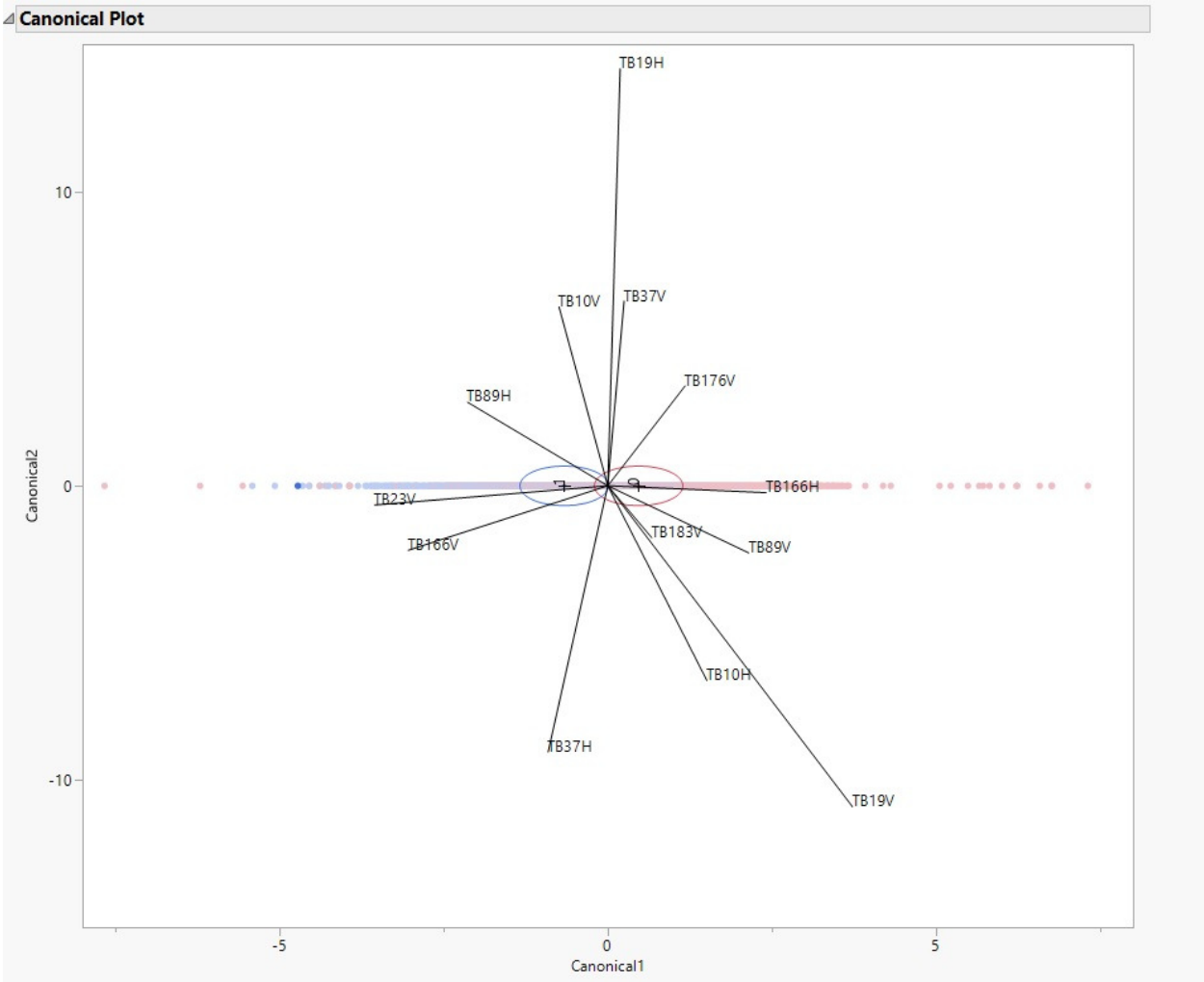

***Figure**: Canonical plot for a linear discriminant regression using all predictors. The points in blue have snowcode 1 and the points in red have snowcode 0.*

(*POC: C. Kongoli, cezar.kongoli@noaa.gov, Funding: CISESS Task I)*